

UNCERTAINTY OF SHIP HULL GIRDER ULTIMATE STRENGTH IN GLOBAL BENDING PREDICTED BY SMITH-TYPE COLLAPSE ANALYSIS

Reference NO. IJME 1157, DOI: 10.5750/ijme.v164iA2.1157

S Li, University of Strathclyde, UK, **D K Kim**, Seoul National University, Korea, **J W Ringsberg**, Chalmers University of Technology, Sweden, **B Liu**, Wuhan University of Technology, China and **S D Benson**, Newcastle University, UK

KEY DATES: Submitted: 13/12/21; Final acceptance: 05/10/22; Published: 30/11/22

SUMMARY

The engineering modelling of ship hull girder strength consists of global and local levels. The Smith-type progressive collapse analysis is a typical example of this, in which the global model requires input from the local model to describe the underlying local structural behaviour, i.e., load-shortening curve (LSC). However, the modelling is prone to uncertainty due to the statistical variability of the basic variables (aleatoric uncertainty) and the inadequacy of engineering models in both global and local levels (epistemic uncertainty). The former can be well tackled by a probabilistic sampling, whereas dealing with the latter for ship hull girder strength lacks an established approach. There can be different sources of epistemic uncertainty. In the modelling of ship hull girder strength, this may be partially manifested as that caused by different choices of local engineering models for predicting the LSC. In light of this, a novel probabilistic method is applied in this research to quantify the uncertainty related to the local models, i.e., the combined computational uncertainty of ultimate compressive strength and post-collapse strength of structural elements. The adopted approach is a hybrid method incorporating the Smith-type progressive collapse method with Monte-Carlo Simulation and an adaptable LSC algorithm. Case studies are performed for the first time on four merchant ships under both uni-axial and bi-axial bending load cases. It is shown that the ultimate strength in sagging is subjected to the most significant computational uncertainty as compared with those in hogging and horizontal bending. In a bi-axial load case, the computational uncertainty estimated for vertical bending will be counteracted as the horizontal bending increases. Nevertheless, this change is not directly proportional to the bi-axial load component ratio and appreciably varies between different ship types. The insights and data provided by this study may eventually resolve the epistemic uncertainty in ship hull girder strength estimation so that improving the ultimate limit state-based reliability analysis.

NOMENCLATURE

A_i	Cross-sectional area of structural element
D_{HH}	Horizontal bending stiffness
D_{VV}	Vertical bending stiffness
D_{HV}	Horizontal and vertical bending interactive stiffness
D_{VH}	Vertical and horizontal bending interactive stiffness
\bar{E}_{T_0}	Initial stiffness of structural element
\bar{E}_T	Instantaneous stiffness of structural element
k_i	Tangent stiffness of structural element
M_H	Horizontal bending moment
M_V	Vertical bending moment
y_G	Horizontal centroid of the neutral axis of ship hull girder cross section
y_i	Horizontal coordinate of structural element
z_G	Vertical centroid of the neutral axis of ship hull girder cross section
z_i	Vertical coordinate of structural element
α	Load component ratio
β	Plate slenderness ratio
χ_H	Horizontal bending curvature
χ_V	Vertical bending curvature
λ	Column slenderness ratio

$\sigma_{1.5\epsilon_{xu}}$	Post-collapse strength of structural element at $1.5\epsilon_{xu}$
$\sigma_{2.0\epsilon_{xu}}$	Post-collapse strength of structural element at $2.0\epsilon_{xu}$
σ_{xu}	Ultimate compressive strength of structural element
σ_x	Compressive stress of structural element in longitudinal direction
σ_{Yeq}	Equivalent material yield stress
ϵ_x	Compressive strain of structural element in longitudinal direction
ϵ_{xe}	Linear limit of structural element
ϵ_{xu}	Ultimate compressive strain of structural element
ϵ_{Yeq}	Equivalent material yield strain

1. INTRODUCTION

The maritime sector has a significant societal impact, from transportation, and energy supply to fishing and leisure. The blue economy is one of the most important elements in modern society. To ensure safe operations of all activities encompassed in this industry, greater attention to the structural integrity of maritime infrastructures is required. In this regard, a robust and accurate prediction of the structural capacity and consequence in extreme condition is highly relevant.

The structural consequences under extreme conditions are inevitably volatile, uncertain, complex, and ambiguous (VUCA). As highlighted by Paik (2020), VUCA may be managed or minimised by improving the engineering model, establishing relevance between random variables, developing historical databases, or completing statistical data analyses. Research in the ultimate strength of ship hull girder is an example where VUCA is relevant. An acceptable global ultimate strength of hull girders is one of the most critical criteria for the structural safety assessment of ship hull structures according to the contemporary ultimate limit state (ULS) philosophy (Paik, 2020; Paik, 2018; Paik and Melchers, 2008; Paik and Thayamballi, 2007). In the past fifty years, several computational methodologies have been proposed to calculate the ship hull girder's ultimate strength. Despite numerous advancements in the engineering models for calculating the ultimate bending strength of ship hull girders, a discrepancy continues to exist between the theoretical estimation and the true value as a result of VUCA. Whilst mitigating VUCA can be extremely difficult, and its quantification is of great importance. The present research is dedicated to tackling the uncertainty aspect. As shown in Figure 1, the uncertainty in the engineering modelling of ship hull girder strength may be caused by the statistical variability of the basic variables (aleatoric uncertainty) and the inadequacy of engineering models in both global model and local model levels (epistemic uncertainty). The basic variables involved in the calculation of ultimate ship hull girder strength generally include:

- Material properties
- Geometric dimensions
- Geometric imperfection shapes
- Geometric imperfection magnitudes
- Welding residual stress
- Load combinations and interactions
- Effects of temperature on material properties
- Age-related degradation
- Accidental damage

These variables can be described as deterministic or random variables that mostly apply at the local panel level but contribute to and influence the overall hull girder strength. Significant efforts have been devoted by researchers worldwide to better quantifying the statistical characteristics of these variables, and the corresponding probabilistic approaches to model the ultimate hull girder strength (Gong and Frangopol, 2020; Liu and Frangopol, 2018; Guedes Soares and Teixeira, 2000; Gaspar et al., 2016; Parunov and Guedes Soares, 2008; Parunov et al., 2020; Teixeira and Guedes Soares, 2009; Xu et al., 2015). The aleatoric uncertainty can be appropriately evaluated for the ship hull girder strength if the statistical variations are well defined. Therefore, this is not in the scope of the present research.

However, the evaluation of epistemic uncertainty is still lacking an established approach. As a measure of the

inadequacy of engineering models, the epistemic uncertainty may be assessed by comparing the theoretical prediction with a corresponding physical measurement. For hull girder collapse, this involves a comparison between a calculated global hull girder strength prediction and an actual collapse test measurement. This is impractical for most full-scale situations and is costly even at a small laboratory scale, where the conditions are also not wholly representative of an actual hull girder collapse event. Such a comparison would also require a thorough knowledge of the true value of the basic variables, which can then be incorporated into the theoretical calculation. This is still fraught with uncertainty and difficulty, as recently shown in Ringsberg et al. (2021), where a tightly controlled benchmark study of a stiffened panel collapse showed continued uncertainty in comparison to the equivalent physical test even with accurate measures of geometrical and material properties. Due to these difficulties, most previous studies of this type either empirically adopted a probabilistic model (e.g., normal distribution) or simply ignored it.

The epistemic uncertainty can be induced not only by the inadequacy of the global engineering model, but also by the local model or engineering representation of the sub-structures. In hull girder strength assessment, it may be resolved by analysing the uncertainty caused by different choices of local engineering model for the stiffened panels, for example, the Load Shortening Curve (LSC) representation within a Smith-type progressive collapse calculation. This is termed as “computational uncertainty” hereafter. A thorough analysis of the computational uncertainty induced by the local engineering model, which takes the form of LSCs, may provide a tangible estimate of the epistemic uncertainty, which could ultimately improve the reliability and risk assessment of ship hull structures.

This research builds on several previous studies. Li et al. (2020a) identified that the ultimate compressive strength and the post-collapse decay within LSCs are the most influential features to the ship hull ultimate strength. Based on this study, a probabilistic approach was proposed to assess the computational uncertainty (Li et al., 2021a). The probabilistic evaluation is driven by Monte-Carlo sampling on the probability distributions of critical LSC features that were developed based upon the comparison between several design formulae and nonlinear finite element analysis (Lin, 1985; Paik and Thayamballi, 1997; Zhang and Khan, 2009; Kim et al., 2017; Kim et al., 2019; Xu et al., 2018).

An adaptable LSC algorithm is utilised to formulate the LSC at each sampling, which is input to the Smith-type progressive collapse analysis. The largest benefit of this method is that the local modelling can be parameterised by the critical LSC features (e.g., ultimate compressive strength and post-collapse unloading), in which case appropriate probability distributions can be assigned and allowing for a probabilistic sampling following the same philosophy of that to deal with the aleatoric uncertainty.



Figure 1. Overview of the uncertainty in the ultimate strength of ship hull girder

This paper is a continuing work with contributions on 1) quantifying the combined effects of ultimate compressive strength and post-collapse characteristics of structural components; 2) extending the loading scenario to bi-axial bending cases. The remainder of this paper is organised as follows: Section 2 supplements the background knowledge related to uncertainty quantification and the ultimate strength of ship hull girders. Section 3 introduces the applied probabilistic method. Section 4 reports the analysis results, and Section 5 discusses the potential future applications of the probabilistic method and the present analysis results. Conclusions and aspects open to further improvement are documented in Section 6.

2. BACKGROUND

In this section, the general concepts of VUCA, uncertainty quantification in engineering problems and ship hull girder strength are introduced.

2.1 VUCA ENVIRONMENTS

The structural safety study in association with extreme conditions is inevitably volatile, uncertain, complex, and ambiguous (VUCA), which was firstly used in 1987 from the leadership theories of Bennis and Nanus. Recently, it is also highlighted by Paik (2020) by linking it with structural safety.

- **Volatility**, which relates to the rapid and dynamic change of the random variables. It can be managed by the relevance of random variables in mathematical models representing a system's behaviour.
- **Uncertainty**, which can be categorised by inherent uncertainty and modelling uncertainty. The inherent uncertainty relates to the natural variabilities in environmental actions and material properties that can be determined by statistical analysis of big data. The modelling uncertainty is caused by the inaccuracy of engineering modelling, and this shall be managed by advanced computational modelling techniques.
- **Complexity**, which is due to many influential factors that are highly nonlinear and do not follow Gaussian aspects. This may be controlled by advanced computational models that suit the computational capacity or modern hardware and software.
- **Ambiguity**, which is resulted by the difficulty in clarifying and manifesting an extreme condition. This can be minimised by processing big databases, including historical and artificial data.

2.2 CLASSIFICATION OF UNCERTAINTY

Uncertainty in an engineering model is commonly defined as a combination of aleatoric uncertainty and epistemic uncertainty. These are elaborated in the following (Matthies 2007; Kiureghiana and Ditlevsen 2009):

- **Aleatoric uncertainty**, also known as inherent uncertainty, which refers to the unknowns that would differ in each experiment. Aleatoric uncertainties exist and cannot be suppressed by more accurate measurements. For example, the variability of material property and geometry dimensions etc are typical aleatoric uncertainties.
- **Epistemic uncertainty**, also known as modelling uncertainty, which is caused by things we could in principle know but do not in practice. This is likely because we have not measured a quantity sufficiently accurately, or because our model neglects certain effects, or because particular data are deliberately hidden.

In real-life applications, both kinds of uncertainties are often present. Uncertainty quantification intends to work toward reducing epistemic uncertainties to aleatoric uncertainties. The quantification for the aleatoric uncertainties is relatively straightforward to perform. Techniques such as the Monte Carlo method are frequently used. A probability distribution can be represented by its moments (in the Gaussian case, the mean and covariance suffice), or more recently, by techniques such as Karhunen-Loève and polynomial chaos expansions. To evaluate epistemic uncertainties, efforts are made to gain better knowledge of the system, process, or mechanism. Methods such as fuzzy logic or evidence theory (Dempster-Shafer theory) are used.

In fact, other classification also exists which are introduced in the following. One of the alternatives to categorise the sources of uncertainty is to consider (Kennedy and O'Hagan 2001):

- **Parameter uncertainty**, which comes from the parameters input to the mathematical model. The exact values of these parameters are unknown and cannot be controlled in physical experiments. Geometry, imperfection and residual stress are the typical examples of this kind. In relation to the common way of classification, the parameter uncertainty may be of the same nature of aleatoric uncertainty.
- **Structural uncertainty**, also known as model inadequacy, model bias, or model discrepancy, which comes from the lack of knowledge of the underlying true physics. It depends on how accurately a mathematical model describes the actual system for a real-life process. In relation to the common way of classification, the structural uncertainty may be of the same nature of epistemic uncertainty.
- **Algorithmic uncertainty**, also known as numerical uncertainty, which comes from numerical errors and numerical approximations per implementation of the computer model. Uncertainty due to different techniques of discretisation in computational methods such as finite element analysis or semi-analytical methods. Smith method may fall into this category.

2.3 SHIP HULL GIRDER STRENGTH

As one of the most critical design criteria in ship structural design, the direct calculation of the ultimate strength of a ship's hull girder in global bending has experienced much advancement since the 1960s. Analysis methods are categorised as:

- Empirical methods
- Presumed stress distribution methods
- Smith-type progressive collapse methods
- Intelligent Supersize Finite Element Method (Based on Idealised Structural Unit Method)
- Nonlinear finite element methods

The empirical method refers to simple regression formula, such as that proposed by Lin (1985), which may serve as a first-cut estimation. Presumed stress distribution methods are developed based on prescribed stress distribution of the ship hull girder cross section in the collapse state, in which the ultimate bending moment is computed by taking the first moment of the resultant stress (Caldwell, 1965; Paik and Mansour, 1995; Paik et al., 2013). The Intelligent Supersize Finite Element Method (ISFEM) was developed by Paik (2006), which improves the computational inefficiency of conventional finite element analysis by introducing large-scale computationally efficient elements (Kim et al., 2012, 2015; Paik et al., 2009; Youssef et al., 2016). The smith-type progressive collapse method was initially introduced by Smith (1977). As a generalisation of the elementary beam theory, it computes the hull girder strength by accounting for the progressive collapse behaviour of the local components. Advancements to the original Smith method include alternative formulations (Gordo and Guedes Soares, 1996), multi-frame collapse (Benson et al., 2013), torsion (Syrigou et al., 2018), cyclic loading (Li et al., 2020b), local bottom load (Tatsumi et al., 2020) and applications on damaged ships (Li and Kim, 2022). The most sophisticated approach, but also the most computationally demanding, is the nonlinear finite element method. Within the bounds of the geometric representation, this covers all buckling modes that occur in the progressive collapse of ship hull girders (Liu and Guedes Soares, 2020; Liu et al., 2021a, 2021b). However, specialised expertise and experience are required for performing nonlinear finite element analysis. Furthermore, its computational time still imposes a significant burden. Hence, the NLFEM is not the usual choice in the initial design phase.

Whilst all of these methods are capable of predicting the ultimate capacity of ship hull girder in global bending. The latter three are distinct from the first two with their ability to predict the entire progressive collapse behaviour.

The foregoing calculation methods belong to global engineering models. Most of them require input from

a subset of local engineering models. For instance, the empirical and presumed stress distribution methods require estimating the ultimate compressive strength of critical components from the local engineering model. The ISFEM and Smith-type progressive collapse method requires the entire load-shortening response predicted by the local engineering model.

Therefore, in parallel to the development of global engineering models, there is significant progress in the local engineering model as well. Generally, they can be categorised as:

- Analytical methods
- Numerical methods
- Empirical methods

The analytical methods are usually formulated based on the classical structural stability theory, which combines with an appropriate way to consider the plasticity effect. These physics-based analytical methods are generally accurate and computationally efficient. However, their accuracy is also subject to the buckling modes embedded in the formulation. A typical example of analytical methods are Common Structural Rule (CSR), and the various local engineering models incorporated in the computer codes for assessing ship structural strength, e.g., ALPS/ULSAP (Paik et al., 2001), ProColl/Panel (Benson et al., 2015), FABSTRAN (Dow and Smith, 1986), HULLST (Yao and Nikolov, 1991; 1992), ULTSTR (Adamchak, 1982).

Numerical methods, usually based on the nonlinear finite element method (NLFEM), are widely used to investigate the buckling and post-buckling behaviour of stiffened panels under compression. The use of NLFEM enables the evaluation of various parameters of influence, including initial imperfections, secondary loadings, in-service degradations and different materials. NLFEM is now established as a capable method to evaluate the elastoplastic buckling and ultimate strength of ship structures. However, the modelling efforts and computational time of finite element methods are substantial compared with other approaches. In addition, as demonstrated by several ISSC benchmark studies (ISSC, 2000; ISSC, 2012; Ringsberg et al., 2021), the finite element solutions may considerably differ because of the uncertainty in modelling techniques, parameter setting and finite element solvers.

Empirical methods for ship structural strength calculation are normally of a pre-defined and empirical function form, and the coefficients are derived by regression analysis. Examples include the empirical formula developed by Lin (1985), Paik and Thayamballi (1997), Zhang and Khan (2009), Kim et al. (2019) and Xu et al. (2018). However, these formulae can only predict the ultimate capacity of structural components. An empirical approach was recently developed by Li et al. (2021b), which enables the

evaluation of the entire load-shortening curves under the full strain range. There is also another type of empirical method, which is based on a direct interpolation of the database e.g., Downes et al. (2017).

3. METHODOLOGICAL CONSIDERATION

3.1 APPLIED PROBABILISTIC APPROACH

The probabilistic approach proposed by Li et al. (2021a) to evaluate the computational uncertainty consists of four steps:

- Identification of the critical features of LSC (Step 1),
- Database generation (Step 2),
- Development of the probability distributions of critical features of LSC (Step 3)
- The combined Monte-Carlo Simulation (Step 4).

Step 1 to Step 3 contribute to the methodology development and have been completed in the previous study. Step 4 is the primary analysis procedure, which is applied in this study. A flowchart of the analysis approach is shown in Figure 2.

As shown by Li et al. (2020a), the ultimate compressive strength and the post-collapse behaviour were concluded

as the most critical characteristics, and thus, their effects on the ultimate strength of ship hull girders were the research object of this study.

The probability density functions of the ultimate compressive strength and the post-collapse strength suggested by Li et al. (2021a) are shown in Figure 3. Further explanation of these LSC features will be provided in Section 3.3. The expressions of all relevant probability density functions are summarised in the Appendix. The development of these probabilistic models follows the procedure adopted by Kim et al. (2019b). The underlying dataset was sub-divided into four sub-domains based on plate slenderness ratio and column slenderness ratio (Domain 1: $\beta > 1.9$ and $\lambda \leq 0.6$; Domain 2: $\beta > 1.9$ and $\lambda > 0.6$; Domain 3: $\beta \leq 1.9$ and $\lambda \leq 0.6$; Domain 4: $\beta \leq 1.9$ and $\lambda > 0.6$). Thus, probability distributions vary with structural configurations, which aims to provide more representative probabilistic models for the critical LSC features.

The combined Monte-Carlo Simulation in Step 4 refers to an integration between the Monte-Carlo sampling and the Smith-type progressive collapse method. At each sampling, the ultimate compressive strength and post-collapse strength are sampled from their probability distributions to formulate an LSC using an adaptable algorithm. This will then be implemented in a Smith-type method, giving a sampled prediction of the ultimate ship hull girder strength. In this study, 800 direct Monte-Carlo samplings will be completed for each load case. As indicated by the convergence test shown in Figure 4, the coefficient of variation (COV) of the ultimate ship hull girder strength converges approximately at 800 samplings. Thus, this is selected as a trade-off between the total computational time and the accuracy. Alternative sample techniques can be considered to reduce the computational time, such as Latin-Hypercube sampling. However, this is out of the scope of this study.

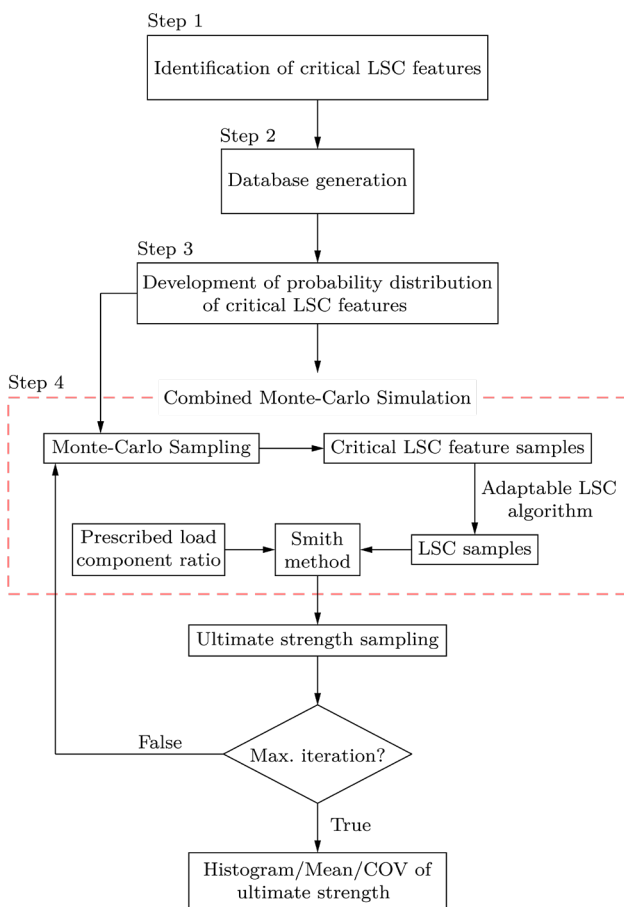


Figure 2. Flowchart of analysis approach

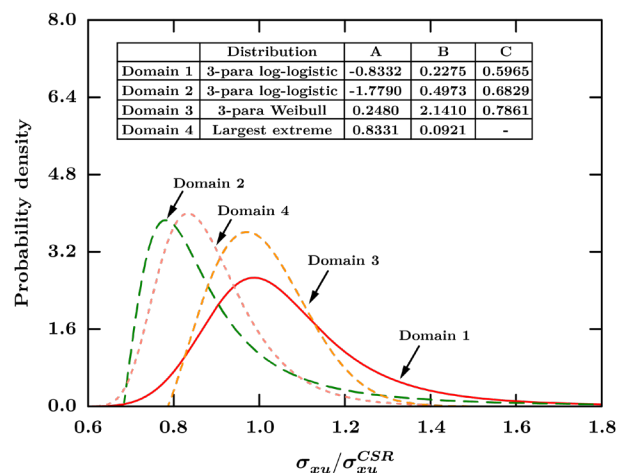


Figure 3(a). Probability density functions of the ultimate compressive strength of local components

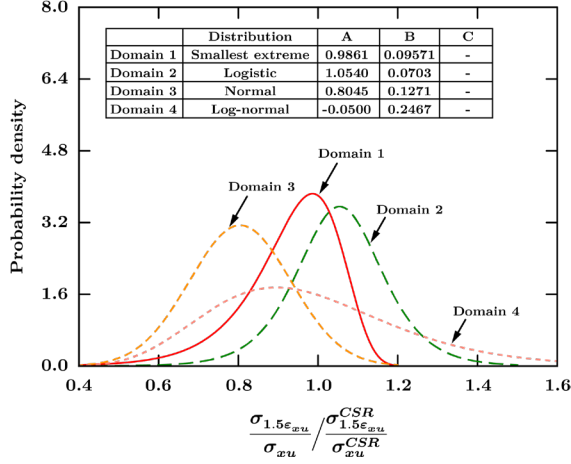


Figure 3(b). Probability density functions of the post-collapse strength at $1.5\epsilon_{xu}$ of local components

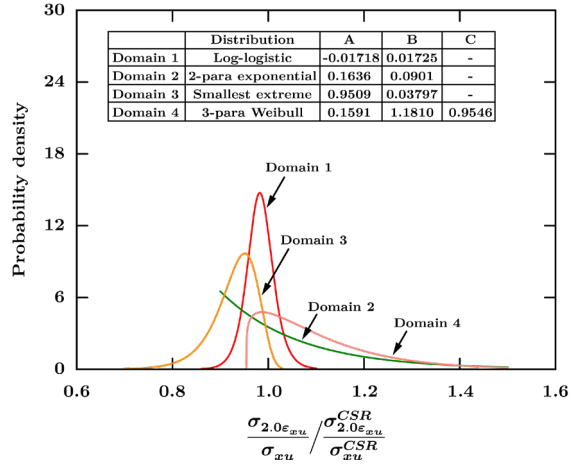


Figure 3(c). Probability density functions of the post-collapse strength at $2.0\epsilon_{xu}$ of local components

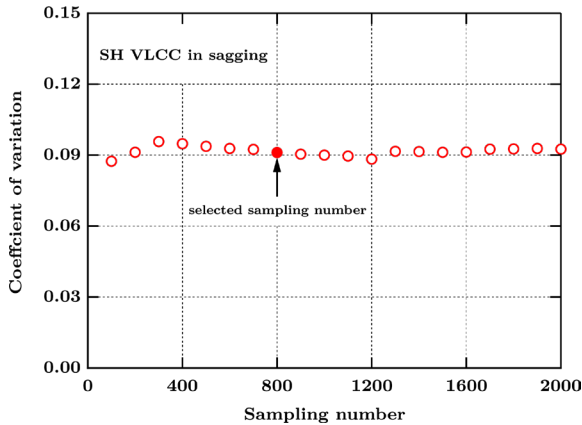


Figure 4. Convergence test of sampling number

3.2 SMITH-TYPE PROGRESSIVE COLLAPSE METHOD

As a generalisation of the Euler-Bernoulli beam theory, the governing equation of the Smith-type method in an

incremental format is given by Equation (1), in which j denotes the current incremental step (Smith, 1977; Dow, 1997; Benson et al., 2013; Li et al., 2020b).

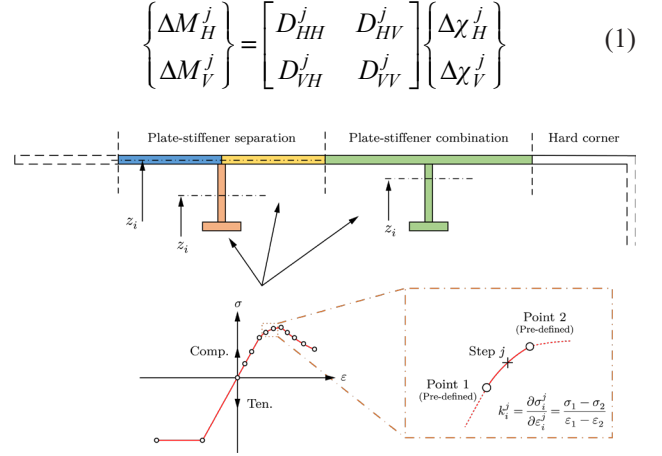


Figure 5. Subdivision of cross section in Smith-type progressive collapse method

In formulating the bending stiffness matrix of Equation (1), a subdivision of the ship hull girder cross section to n structural elements is carried out, as shown in Figure 5, in which a standard plate-stiffener subdivision or a more refined plate-stiffener separation technique can be employed.

Each structural element is assigned with a load-shortening curve, which defines its tangent stiffness k_i^j under compression and tension where i denotes the element number. The tangent stiffness is defined by Equation (2) and is numerically evaluated based on the available data points in the computer code realisation.

$$k_i^j = \frac{\partial \sigma_i^j}{\partial \epsilon_i^j} \quad (2)$$

The bending stiffness matrix is assembled following Equation (3).

$$D_{HH}^j = \sum_{i=1}^n k_i^j A_i (y_i - y_G^j)^2 \quad (3a)$$

$$D_{VV}^j = \sum_{i=1}^n k_i^j A_i (z_i - z_G^j)^2 \quad (3b)$$

$$D_{HV}^j = D_{VH}^j = \sum_{i=1}^n k_i^j A_i (y_i - y_G^j)(z_i - z_G^j) \quad (3c)$$

These relationships are effectively an adaptation of the parallel axis theorem where the elastic modulus is replaced by the tangent stiffness, and the own inertia of each element is neglected. This neglect could be justified by the fact that the principal dimension of a ship hull cross section is much larger than the scantling of individual

structural elements. Thus, its own inertia has a negligible contribution to the overall bending capacity.

As Fujikubo et al. (2012) introduced, the solution to Equation (1) may be obtained via a prescribed curvature ratio or a prescribed moment ratio approach. In this study the latter is adopted, which is written as Equation (4) to Equation (6).

$$\begin{Bmatrix} a\Delta M_V^j \\ \Delta M_V^j \end{Bmatrix} = \begin{bmatrix} D_{HH}^j & D_{HV}^j \\ D_{VH}^j & D_{VV}^j \end{bmatrix} \begin{Bmatrix} \Delta \chi_H^j \\ \Delta \chi_V^j \end{Bmatrix} \quad (4)$$

$$\Delta M_V^j = \frac{\Delta M_H^j}{a} = \frac{D_{HH}^j D_{VV}^j - D_{HV}^j D_{VH}^j}{D_{HH}^j - a D_{VH}^j} \Delta \chi_V^j \quad (5)$$

$$\Delta \chi_H^j = \frac{a D_{VV}^j - D_{HV}^j}{D_{HH}^j - a D_{VH}^j} \Delta \chi_V^j \quad (6)$$

This technique is employed since the ultimate ship hull girder can be directly obtained without an iterative search. It should be noted that both solution schemes utilise curvature as the controlling parameter. Alternatively, the bending moment can be chosen, in which case the maximum capacity is determined when the solution breaks down. However, this is not able to predict post-collapse behaviour.

At each increment, the neutral axis position of the cross section will be translated and rotated due to the loss in tangent stiffness of structural components. Thus, its centroid (y_G, z_G) should be updated in accordance with Equation (7), which are derived by the first moment of area of the cross section considering the progressive collapse effects.

$$y_G = \sum_{i=1}^n y_i k_i^j A_i / \sum_{i=1}^n k_i^j A_i \quad (7a)$$

$$z_G = \sum_{i=1}^n z_i k_i^j A_i / \sum_{i=1}^n k_i^j A_i \quad (7b)$$

To drive the update of cross-sectional neutral axis position and tangent stiffened of the local element, the incremental strain of each local element is computed as follows:

$$\Delta \varepsilon_i^j = \Delta \chi_H^j (y_i - y_G^j) + \Delta \chi_V^j (z_i - z_G^j) \quad (8)$$

3.3 ADAPTABLE LOAD-SHORTENING CURVE FORMULATION

For the probabilistic evaluation of the effects of load-shortening curve (LSC) on hull girder strength calculation, the adaptable algorithm developed by Li et al. (2021b) is adopted. This algorithm is developed based on the idealisation of the prediction by the nonlinear finite element method. It predicts the compressive LSC from four critical

features: elastic stiffness, ultimate compressive strength, ultimate strain and an asymptotic post-collapse decay. Each of these critical features can be modified for specific characteristics. The elastic stiffness is usually assumed as the elastic modulus of the material. The ultimate compressive strength can be predicted by any empirical formula and/or the more elaborated numerical simulation (e.g., nonlinear finite element method). A schematic illustration of the adaptable algorithm is given in Figure 6, and the complete expressions of the adaptable algorithm are given as Equation (9).

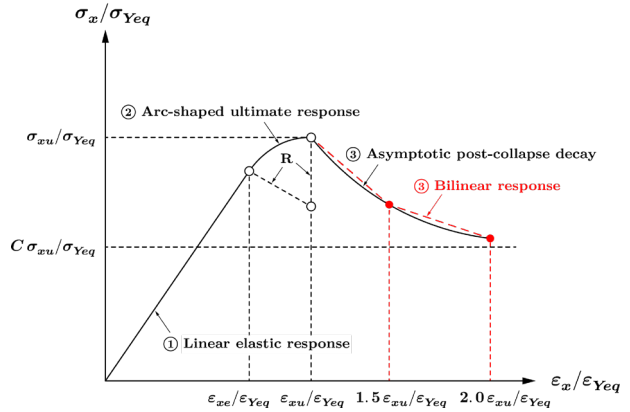


Figure 6. Schematic illustration of the adaptable algorithm to predict the load-shortening curve

If $\varepsilon_x / \varepsilon_{Yeq} \leq \varepsilon_{xe} / \varepsilon_{Yeq}$

$$\frac{\sigma_x}{\sigma_{Yeq}} = \bar{E}_{T_o} \frac{\varepsilon_x}{\varepsilon_{Yeq}} \quad (9a)$$

else if $\varepsilon_{xe} / \varepsilon_{Yeq} < \varepsilon_x / \varepsilon_{Yeq} < \varepsilon_{xu} / \varepsilon_{Yeq}$

$$\frac{\sigma_x}{\sigma_{Yeq}} = \frac{\sigma_{xu}}{\sigma_{Yeq}} - R + R \cos \left[-\tan^{-1} \left(\bar{E}_T \right) \right] \quad (9b)$$

else if $\varepsilon_{xu} / \varepsilon_{Yeq} \leq \varepsilon_x / \varepsilon_{Yeq} < 1.5\varepsilon_{xu} / \varepsilon_{Yeq}$

$$\frac{\sigma_x}{\sigma_{Yeq}} = \frac{\sigma_{xu}}{\sigma_{Yeq}} + \bar{E}_{p1} \left(\frac{\varepsilon_x}{\varepsilon_{Yeq}} - \frac{\varepsilon_{xu}}{\varepsilon_{Yeq}} \right) \quad (9c)$$

else if $\varepsilon_x / \varepsilon_{Yeq} \geq 1.5\varepsilon_{xu} / \varepsilon_{Yeq}$

$$\frac{\sigma_x}{\sigma_{Yeq}} = \frac{\sigma_{1.5\varepsilon_{xu}}}{\sigma_{Yeq}} + \bar{E}_{p2} \left(\frac{\varepsilon_x}{\varepsilon_{Yeq}} - \frac{1.5\varepsilon_{xu}}{\varepsilon_{Yeq}} \right) \quad (9d)$$

where

$$R = \frac{\cos \left[\tan^{-1} \left(\bar{E}_{T_o} \right) \right] \left(\bar{E}_{T_o} \frac{\varepsilon_{xu}}{\varepsilon_{Yeq}} - \frac{\sigma_{xu}}{\sigma_{Yeq}} \right)}{1 - \cos \left[\tan^{-1} \left(\bar{E}_{T_o} \right) \right]}$$

$$\frac{\varepsilon_{xe}}{\varepsilon_{Yeq}} = \frac{\varepsilon_{xu}}{\varepsilon_{Yeq}} + R \sin \left[-\tan^{-1} \left(\bar{E}_{T_o} \right) \right]$$

$$\bar{E}_{p1} = \left(\frac{\sigma_{1.5\varepsilon_{xu}}}{\sigma_{Yeq}} - \frac{\sigma_{xu}}{\sigma_{Yeq}} \right) / \left(\frac{1.5\varepsilon_{xu}}{\varepsilon_{Yeq}} - \frac{\varepsilon_{xu}}{\varepsilon_{Yeq}} \right)$$

$$\bar{E}_{p2} = \left(\frac{\sigma_{2.0\varepsilon_{xu}}}{\sigma_{Yeq}} - \frac{\sigma_{1.5\varepsilon_{xu}}}{\sigma_{Yeq}} \right) / \left(\frac{2.0\varepsilon_{xu}}{\varepsilon_{Yeq}} - \frac{1.5\varepsilon_{xu}}{\varepsilon_{Yeq}} \right)$$

In this study, only the ultimate compressive strength and the post-collapse decay are probabilistically described, whereas the elastic stiffness and ultimate strain are deterministic. In addition, the post-collapse decay is modified from an asymptotic behaviour to a bi-linear response dominated by the post-collapse strength at $1.5\varepsilon_{xu}$ and $2.0\varepsilon_{xu}$, to facilitate its probabilistic representation and the comparison with the CSR method (IACS, 2019). This simplification is justified by comparing it with the standard CSR approach for an example calculation, as shown in Figure 7.

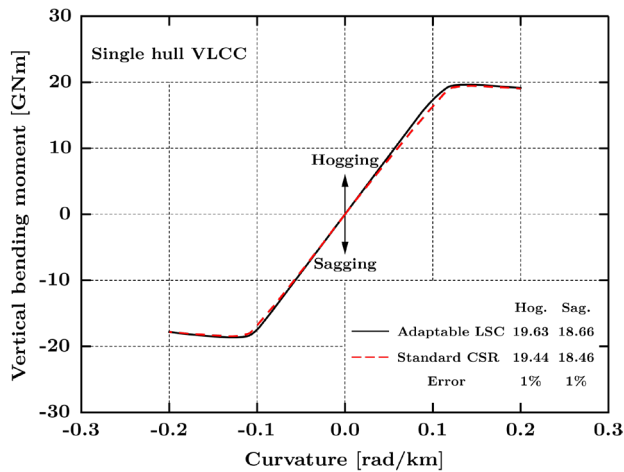


Figure 7. Example comparison of the progressive collapse behaviour predicted by different LSC formulations

4. TEST MATRIX

The analyses are carried out on four case study ships, namely single hull VLCC, double hull VLCC, bulk carrier and container ship (Figure 8) (ISSC, 2000; 2012). The single hull VLCC and double hull VLCC are both closed cross sections. The former is of a single-skin configuration without a longitudinal bulkhead, whereas the latter is of a double-skin design with two longitudinal bulkheads. Additionally, the bulk carrier and the container ship models are open-deck designs with double bottoms. In sagging, the overall collapse of all model types is usually triggered by the buckling of the deck panels. Conversely, in hogging, the first failure normally occurs at the deck panels due

to tensile yielding, but eventually, the overall collapse is induced by the bottom panel buckling. For each case study ship, a total of 19 load cases are analysed, including pure sagging, pure hogging, pure horizontal bending and 16 cases of combined vertical and horizontal bending. It should be noted that, in a normal operational state, the likelihood of the horizontal bending moment becoming dominant or entirely subjected to horizontal bending is relatively low. However, the full analysis is performed as the results may be valuable to an inclined condition due to compartment flooding. Overall, 76 analysis cases are performed, each of which is repeated by 800 times. Thus, a total of 60,800 Smith-type progressive collapse analyses are completed.

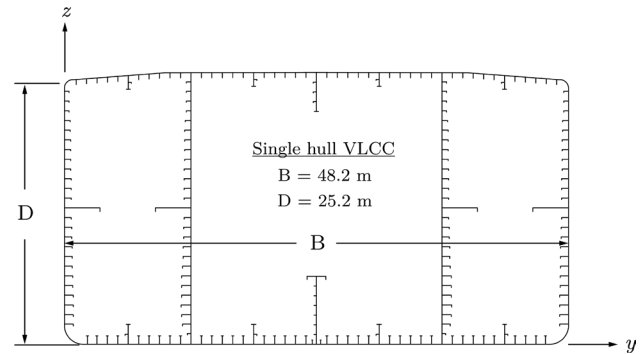


Figure 8(a). Midship cross sections of single hull VLCC

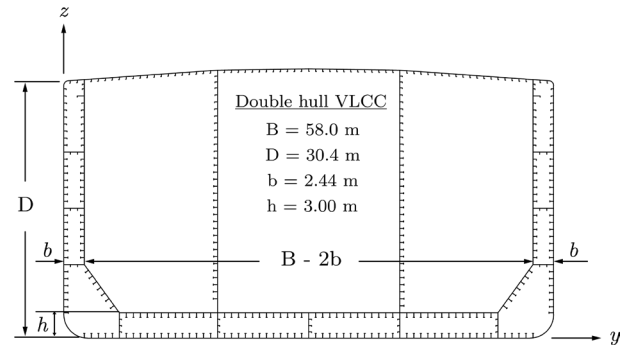


Figure 8(b). Midship cross sections of double hull VLCC

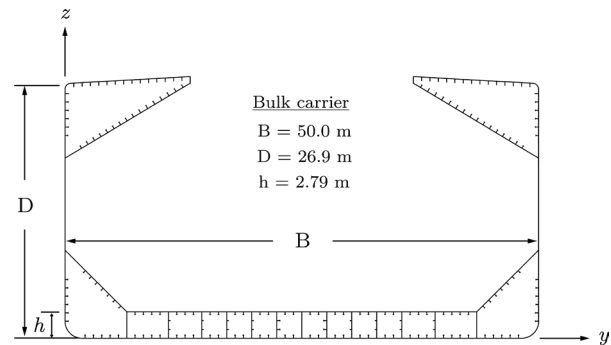


Figure 8(c). Midship cross sections of bulk carrier

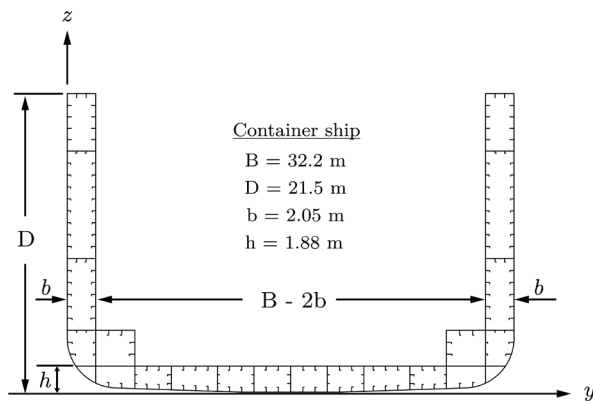


Figure 8(d). Midship cross sections of container ship

5. RESULTS

5.1 UNI-AXIAL BENDING

The histograms of the ultimate ship hull girder strength in uniaxial bending normalised by CSR prediction are shown in Figures 9 to 12 for each case study model, respectively. The ultimate strength is normalised by CSR prediction to provide an indication of the discrepancy with respect to a codified approach, i.e., CSR formulation. The Coefficient of Variation (COV) from a fitted normal distribution curve is taken as a measure of the computational uncertainty and are collated in Table 1. A detailed investigation on their respective influence was reported by Li et al. (2021a). It was shown that the uncertainty of the strength of merchant ships is dominated by the ultimate compressive strength of structural members. By contrast, the uncertainty of the strength of naval ships is caused by both ultimate compressive strength and post-ultimate decay within LSC. In addition, the four critical features of LSC and their impact on computational uncertainty were explored by Li et al. (2020a) in a deterministic manner. Interested readers may refer to the aforementioned publications, and the numerical examples presented

Table 1. Computational Uncertainty (Mean: mean value of the normalised ultimate strength; COV: coefficient of variation)

		Hog	Sag
SH VLCC	Mean	0.98	1.00
	COV	0.06	0.08
DH VLCC	Mean	0.98	0.96
	COV	0.04	0.08
Bulk Carrier	Mean	0.99	0.95
	COV	0.02	0.09
Container Ship	Mean	1.02	0.95
	COV	0.04	0.09

herein consider the combined effect of the uncertainty in ultimate compressive strength and post-collapse strength of structural members.

Larger computational uncertainty is induced when the ship hull girder is subjected to sagging (0.08 to 0.10) compared to hogging (0.02 to 0.06). The largest uncertainty in hogging is the SH VLCC, which is the only cross section without a double bottom arrangement.

The difference between hogging and sagging is due to the relative slenderness in the compressed stiffened panels, in combination with their arrangement, in each loading scenario. In these case studies, the deck panels are slenderer and show larger computational uncertainty at the local level when placed in compression. This propagates greater uncertainty about the hull girder capacity.

The computed strength uncertainty in horizontal bending is also considerable (0.05 to 0.08). In this scenario, the compressive load is imposed on both the deck and bottom panels. For closed cross sections (SH VLCC and DH VLCC), the uncertainty of horizontal bending strength is similar to that of hogging strength. However, for the cross sections with deck opening (bulk carrier and container ship), the uncertainty in horizontal bending is much greater than that in hogging.

The mean value of the normalised ultimate ship hull girder strength enables comparison with CSR. This shows the direct calculations are conservative in all but three cases. The most conservative mean value is found on the horizontal strength of SH VLCC, which is lower than the CSR prediction by 6.3%. The optimistic CSR-based computation may be primarily attributed to the use of the Frankland formula for evaluating the effective width. As compared with the others, such as the Faulkner formula (Faulkner, 1975), the Frankland formula usually overestimates the buckling resistance of local plating since it was developed based on the testing data on constrained plates (Frankland, 1940).

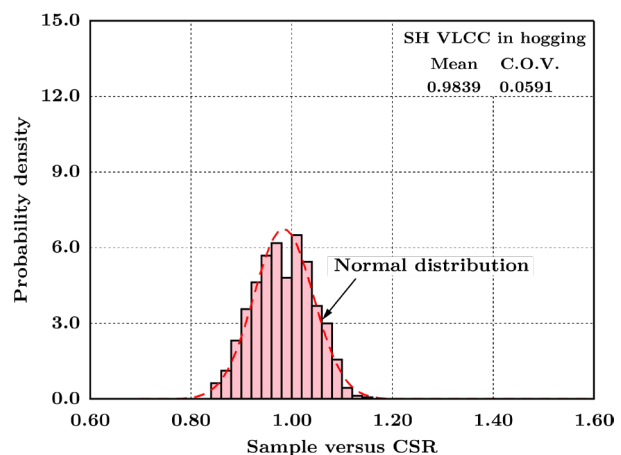


Figure 9(a). Histogram of the normalised ultimate strength (SH VLCC in hogging)

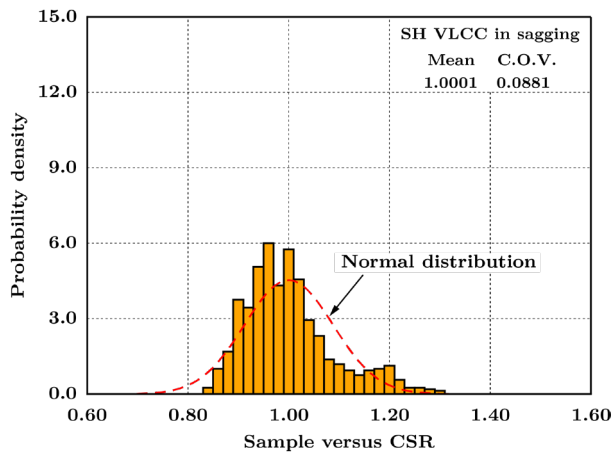


Figure 9(b). Histogram of the normalised ultimate strength (SH VLCC in sagging)

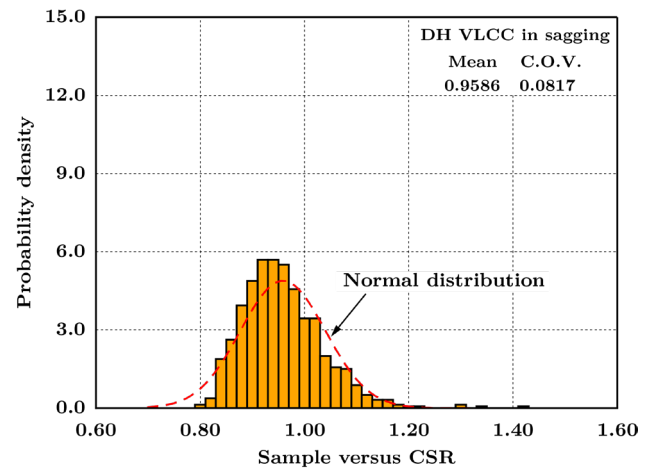


Figure 10(b). Histogram of the normalised ultimate strength (DH VLCC in sagging)

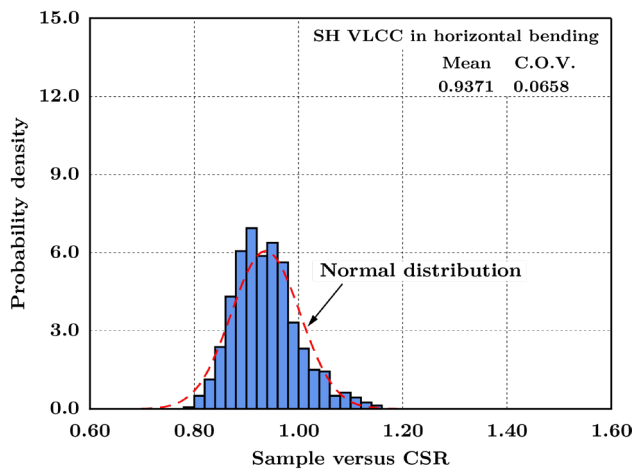


Figure 9(c). Histogram of the normalised ultimate strength (SH VLCC in horizontal bending)

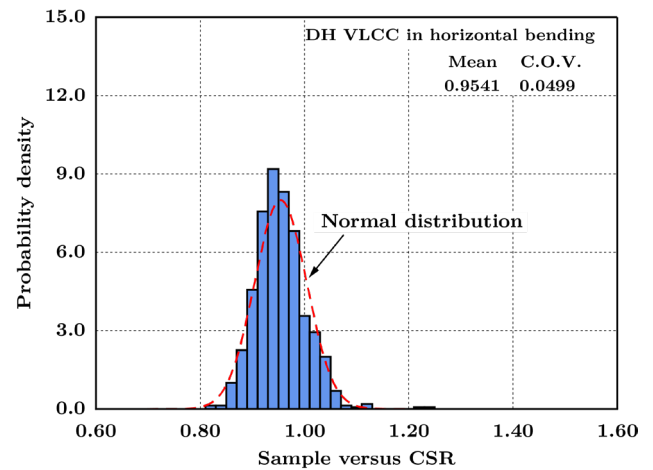


Figure 10(c). Histogram of the normalised ultimate strength (DH VLCC in horizontal bending)

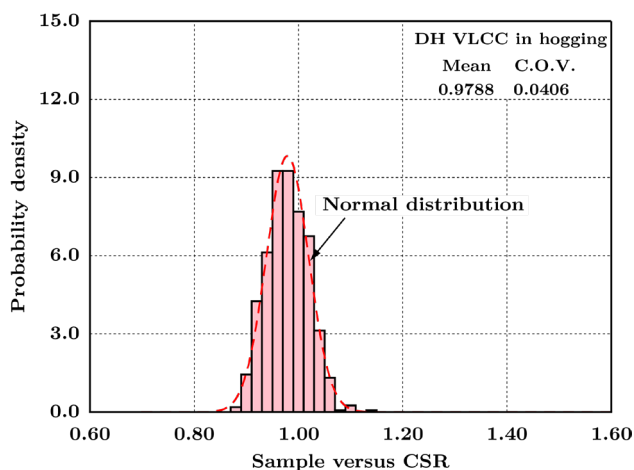


Figure 10(a). Histogram of the normalised ultimate strength (DH VLCC in hogging)

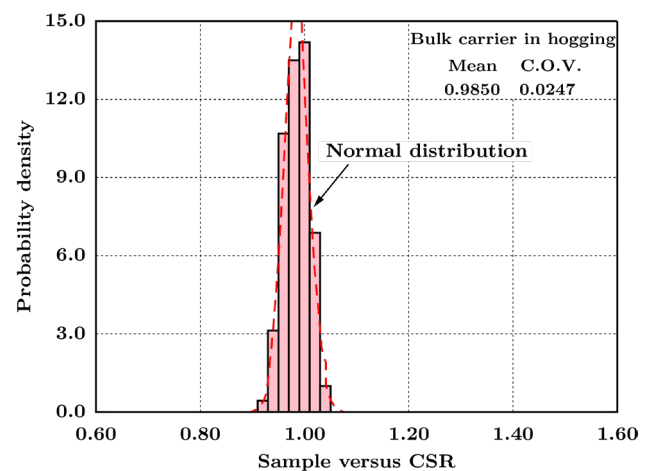


Figure 11(a). Histogram of the normalised ultimate strength (Bulk carrier in hogging)

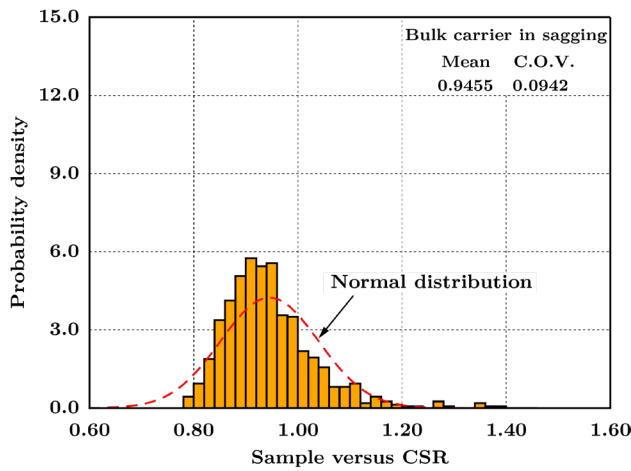


Figure 11(b). Histogram of the normalised ultimate strength (Bulk carrier in sagging)

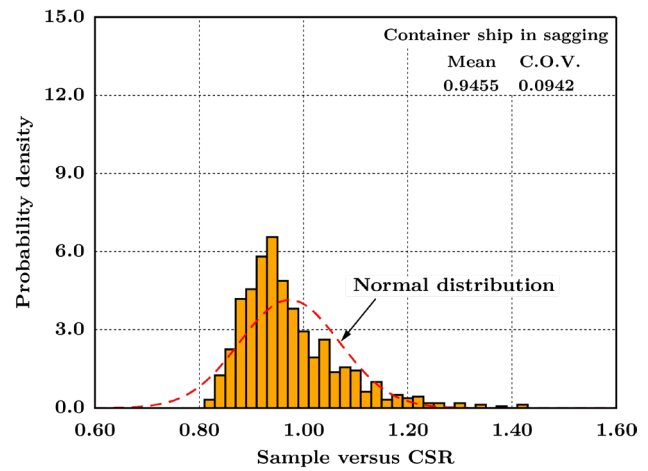


Figure 12(b). Histogram of the normalised ultimate strength (Container ship in sagging)

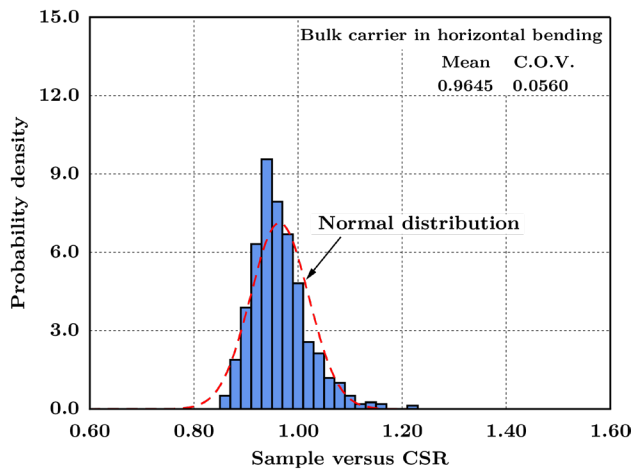


Figure 11(c). Histogram of the normalised ultimate strength (Bulk carrier in horizontal bending)

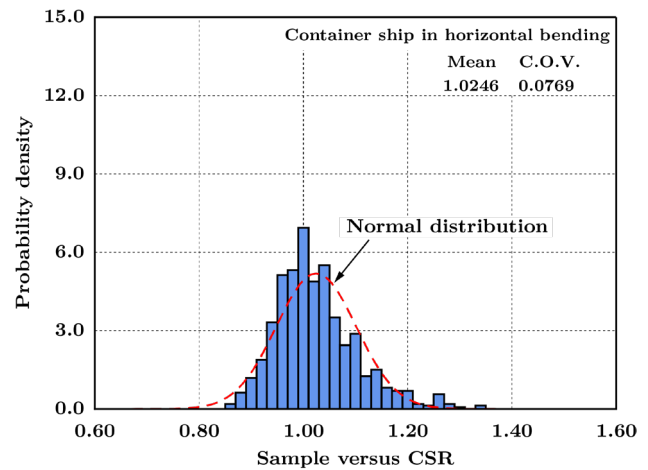


Figure 12(c). Histogram of the normalised ultimate strength (Container ship in horizontal bending)

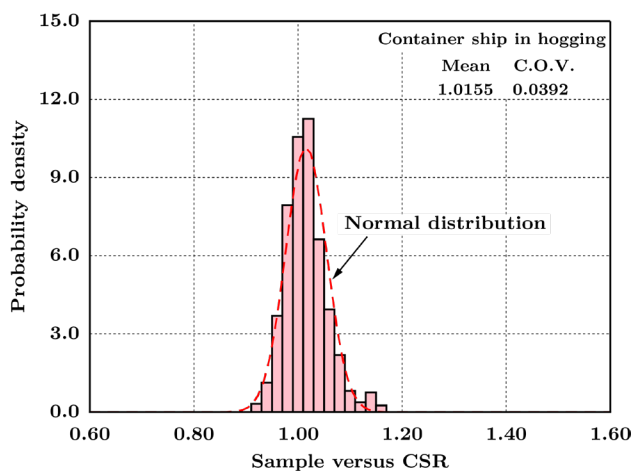


Figure 12(a). Histogram of the normalised ultimate strength (Container ship in hogging)

The difference in the computational uncertainty between different load cases and ship types may also be interpreted in association with the cross-sectional neutral axis translation during progressive collapse (Figure 13). The progressive collapse is mainly driven by the elastoplastic buckling due to compression when the hull girder is submitted to sagging or horizontal bending. Hence, the neutral axis translates substantially away from the collapsed components, which further increases the compressed portion within the cross section. As a result, greater computational uncertainty is developed. However, in terms of hogging load, the collapse also involves the tensile yielding of deck panels, which compensates for the compressive failure and the stiffness loss in the bottom panels. Therefore, the cross-sectional neutral axis would generally remain close to its initial position. However, the neutral axis of an ultra-large container ship in progressive collapse due to hogging (e.g., with a capacity over 16000 TEU) arguably experiences significant translation. Further investigation is required to quantify the computational uncertainty of container ships of different classes.

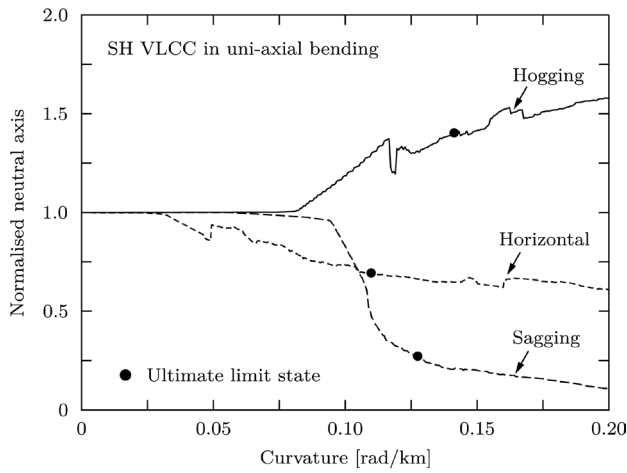


Figure 13(a). Translation of neutral axis during progressive collapse (SH VLCC)

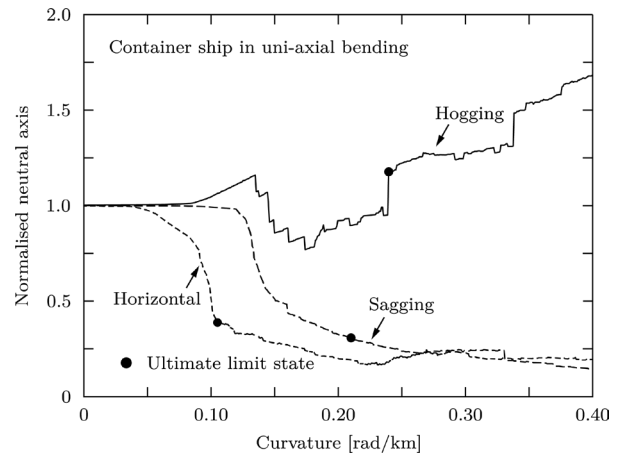


Figure 13(d). Translation of neutral axis during progressive collapse (Container ship)

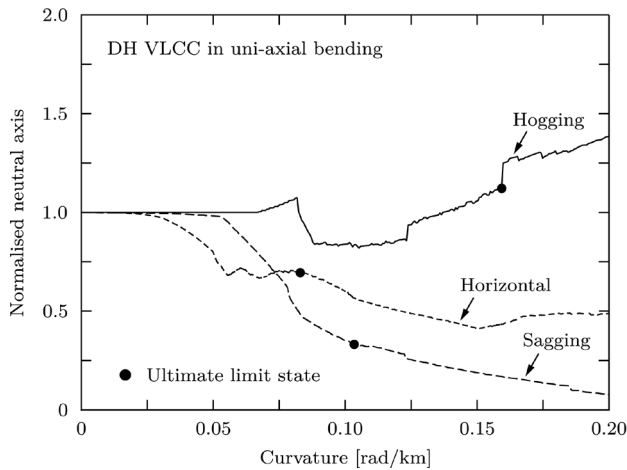


Figure 13(b). Translation of neutral axis during progressive collapse (DH VLCC)

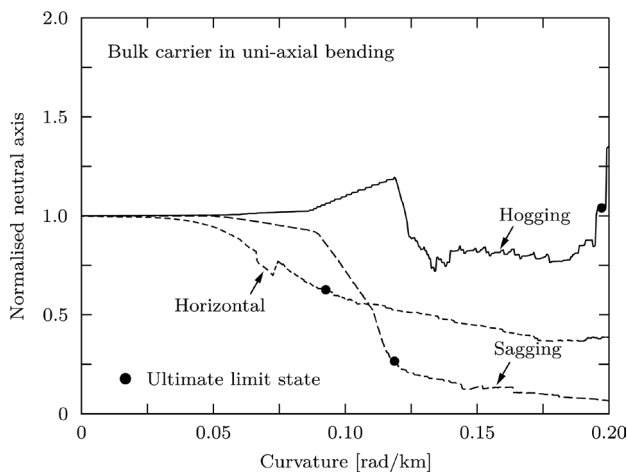


Figure 13(c). Translation of neutral axis during progressive collapse (Bulk carrier)

A comparison of the present results with those reported in ISSC (2000; 2012) is summarised in Tables 2 to 5. All benchmark results are normalised by the corresponding CSR-based estimation. It is notable that the ISSC (2012) shows a larger variation than the ISSC (2000). The COV of hogging strength by the present analysis appears to be underestimated than both ISSC results. However, there is no clear correlation with the sagging strength. In the meantime, the ISSC (2000) also demonstrates a larger variation of the sagging strength than the hogging strength. The discrepancy in the estimation of mean ultimate strength and its COV between the ISSC benchmark studies and the present analysis may be attributed to:

- The sample sizes of the ISSC benchmark studies are considerably smaller than the present analysis. Thus, the mean and COV may only be able to represent the calculation uncertainty among the participants rather than overall statistical performance.
- Several alternative calculation methods other than the Smith-type analysis were adopted in the ISSC benchmarks, including NLFEM with different FE packages and analytical formulas. Uncertainty may thus be induced due to different methodologies. Thus, the uncertainty embedded in the ISSC results is caused by both global and local engineering models, whereas the present study only focuses on the local level.

Table 2. Comparison with ISSC benchmark studies (SH VLCC) (Mean: mean value of the normalised ultimate strength; COV: coefficient of variation)

		Hog	Sag
ISSC (2000)	Mean	0.9784	0.9340
	COV	0.0488	0.0537
ISSC (2012)	Mean	0.9925	0.9747
	COV	0.0897	0.0873
Present	Mean	0.9839	1.0001
	COV	0.0591	0.0881

Table 3. Comparison with ISSC benchmark studies (DH VLCC) (Mean: mean value of the normalised ultimate strength; COV: coefficient of variation)

		Hog	Sag
ISSC (2000)	Mean	1.0346	1.1216
	COV	0.0587	0.1222
ISSC (2012)	Mean	0.9752	1.1388
	COV	0.1263	0.1236
Present	Mean	0.9788	0.9586
	COV	0.0406	0.0817

Table 4. Comparison with ISSC benchmark studies (Bulk carrier) (Mean: mean value of the normalised ultimate strength; COV: coefficient of variation)

		Hog	Sag
ISSC (2000)	Mean	1.0018	1.0055
	COV	0.0469	0.0623
ISSC (2012)	Mean	0.9514	1.0302
	COV	0.0694	0.1178
Present	Mean	0.9850	0.9455
	COV	0.0247	0.0942

Table 5. Comparison with ISSC benchmark studies (Container ship) (Mean: mean value of the normalised ultimate strength; COV: coefficient of variation)

		Hog	Sag
ISSC (2000)	Mean	0.9753	0.9474
	COV	0.0839	0.1507
ISSC (2012)	Mean	0.9776	1.0154
	COV	0.0776	0.0873
Present	Mean	1.0155	0.9734
	COV	0.0392	0.0962

5.2 BI-AXIAL BENDING

A selection of the vertical bending moment versus curvature relationships based on the CSR formulation is shown in Figure 14 for biaxial loading, where the vertical bending is the predominant component.

Generally, the overall progressive collapse behaviours as represented by these curves remain similar with the increase of the horizontal bending since the fundamental load-shortening curves are not changed. The presence of horizontal bending increases the resultant stress on each structural element. Hence the hull girder collapse takes place at a smaller vertical bending moment. In other words, the hull girder has a reduced vertical bending strength.

The interactive diagrams between the vertical and horizontal bending strength are shown in Figure 15. The horizontal axis represents the horizontal bending strength, and the vertical axis indicates the vertical bending strength, both of which are normalised by the corresponding ultimate monotonic strength. These diagrams provide information on the interactive influence between loading components, such as the reduction in vertical bending strength caused by a certain amount of horizontal bending. The interactive relationship is compared between the CSR-based computation and an empirical formula proposed by Paik (2018), which was derived based on the calculation using the intelligent supersize finite element method. The empirical formula is close to the CSR results of the bulk carrier and container ship. However, it is relatively conservative on the single hull VLCC and double hull VLCC. It should be noted that Paik's interactive formula accounted for the effect of welding residual stress.

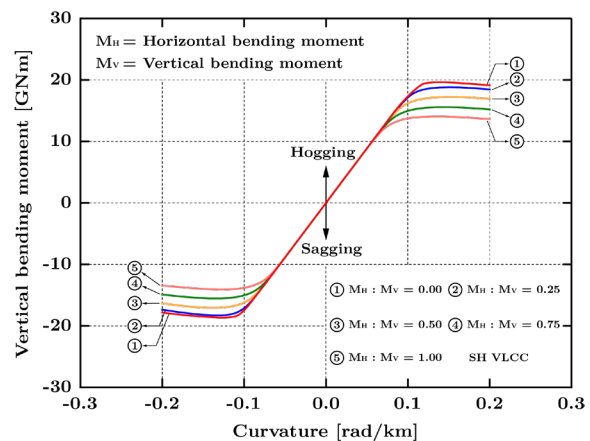


Figure 14(a). Bending moment versus curvature relations in biaxial loading (SH VLCC)

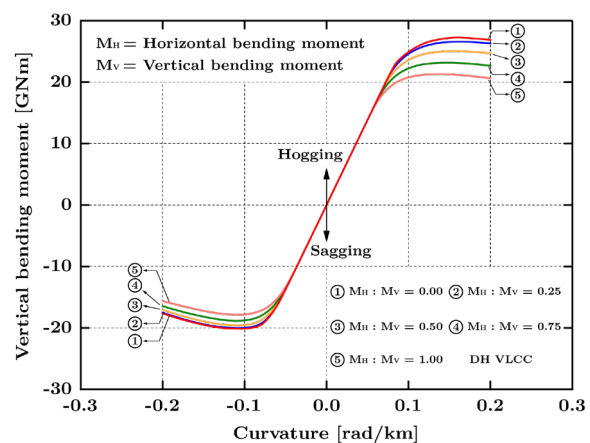


Figure 14(b). Bending moment versus curvature relations in biaxial loading (DH VLCC)

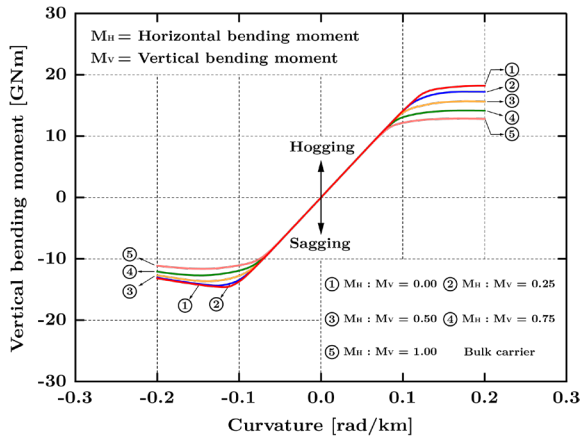


Figure 14(c). Bending moment versus curvature relations in biaxial loading (Bulk carrier)

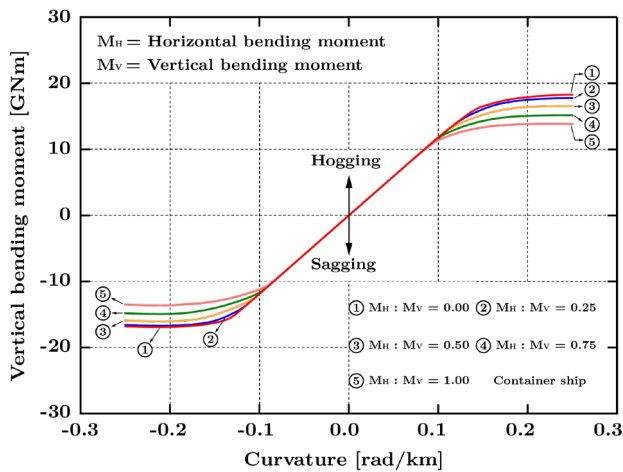


Figure 14(d). Bending moment versus curvature relations in biaxial loading (Container ship)

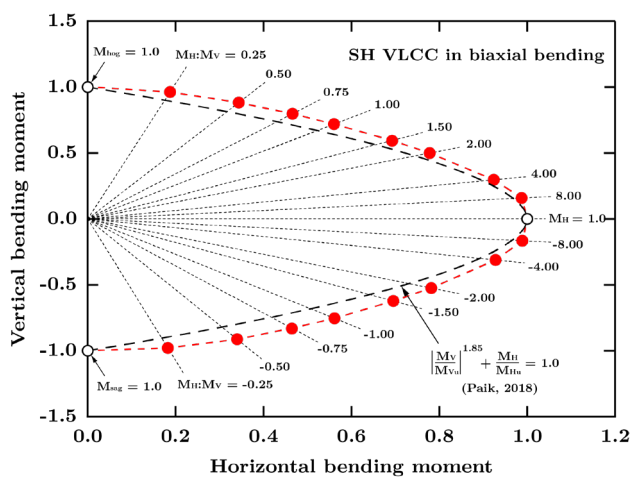


Figure 15(a). Interaction diagram of the ultimate ship hull girder strength in biaxial bending (SH VLCC)

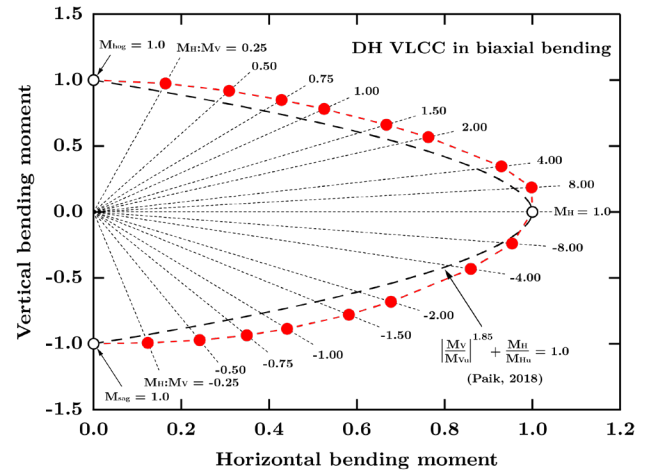


Figure 15(b). Interaction diagram of the ultimate ship hull girder strength in biaxial bending (DH VLCC)

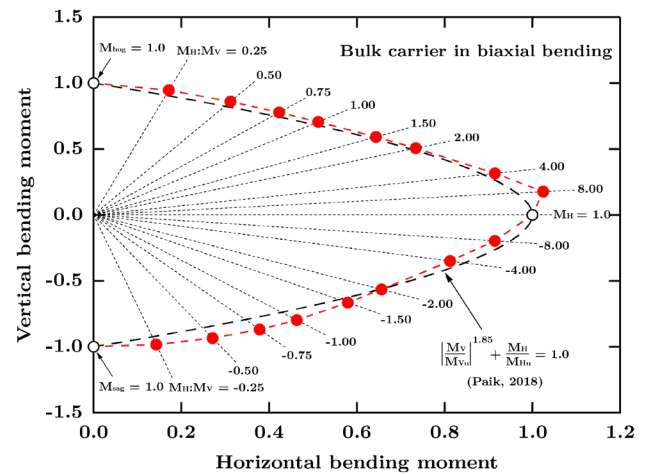


Figure 15(c). Interaction diagram of the ultimate ship hull girder strength in biaxial bending (Bulk carrier)

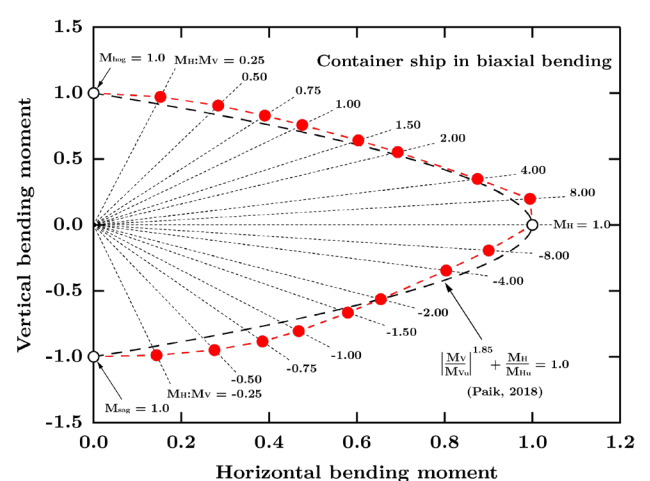


Figure 15(d). Interaction diagram of the ultimate ship hull girder strength in biaxial bending (Container ship)

The variations of the mean ultimate strength in bi-axial bending and its COV are illustrated in Figure 16 to Figure 19. Likely due to the simultaneous translation and rotation of both vertical and horizontal neutral axes, the mean/COV of the normalised ultimate strength is not directly proportional to the load component ratio. With the increase of the horizontal bending, the mean ultimate strength and its COV, in most cases, approach the statistics obtained in pure horizontal bending. Exceptions to this pattern are the mean ultimate sagging strength of bulk carriers and container ships. A decrease of the mean strength is first shown before approaching the statistics obtained in pure horizontal bending. Meanwhile, this variation is also independent of the ship types. For instance, the COV of the sagging strength of single hull VLCC is significantly reduced as soon as the horizontal bending is applied. However, the sagging strength of double hull VLCC is not sensitive to the horizontal bending until the latter becomes the dominating load component. In terms of the difference in the computational uncertainty between sagging and hogging, the COVs of the ultimate hull girder strength approach to a similar value when the biaxial load component is larger than 4.0 and 8.0 for the prismatic cross sections and open-deck cross sections, respectively.

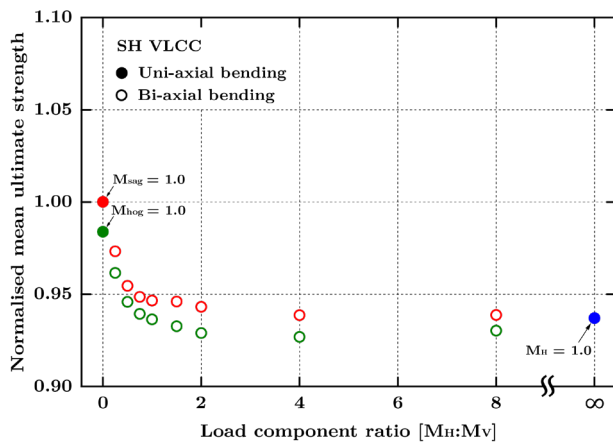


Figure 16(a). Mean ultimate strength under bi-axial load (SH VLCC)

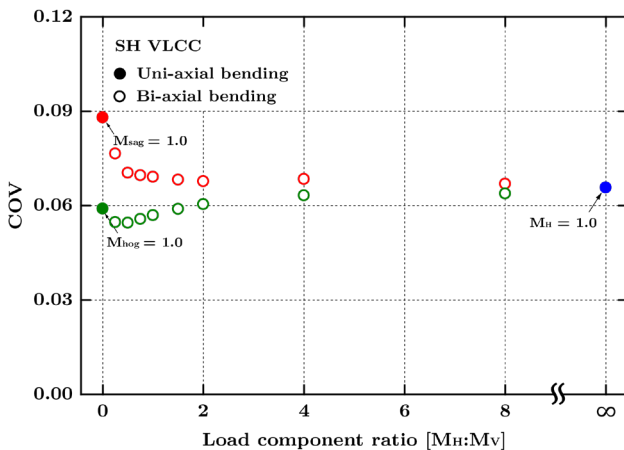


Figure 16(b). Coefficient of variation of ultimate strength under bi-axial load (SH VLCC)

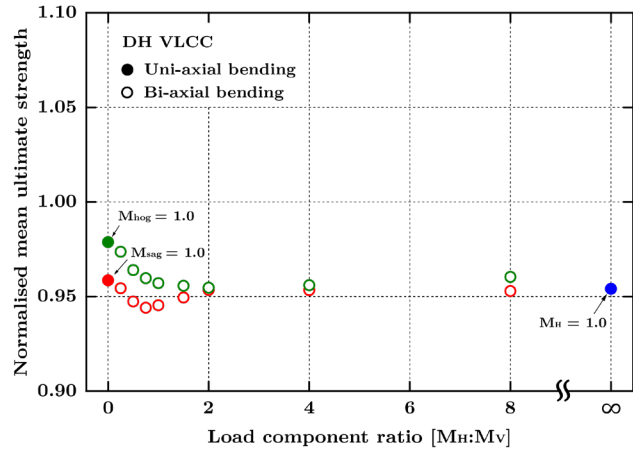


Figure 17(a). Mean ultimate strength under bi-axial load (DH VLCC)

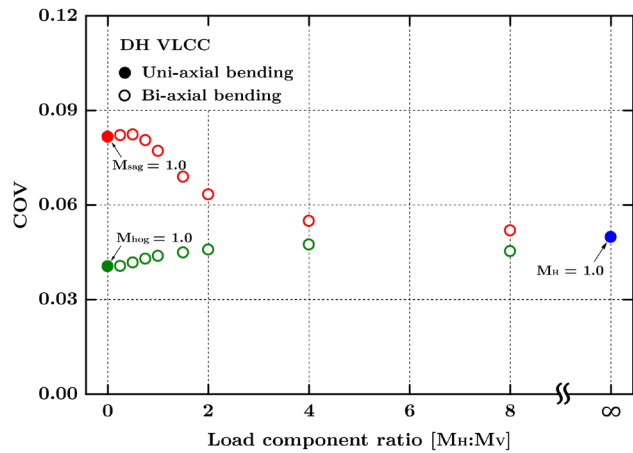


Figure 17(b). Coefficient of variation of ultimate strength under bi-axial load (DH VLCC)

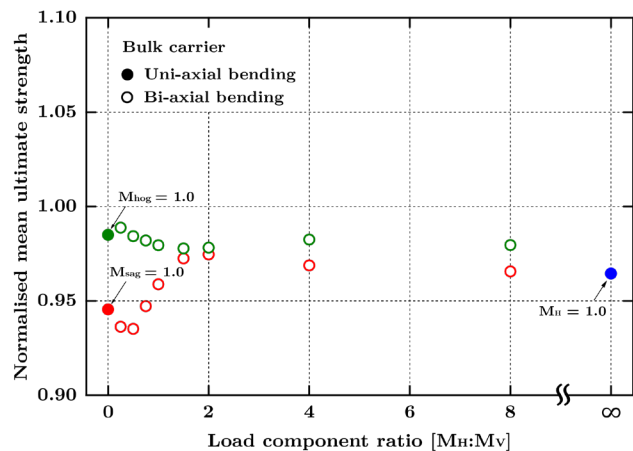


Figure 18(a). Mean ultimate strength under bi-axial load (Bulk carrier)

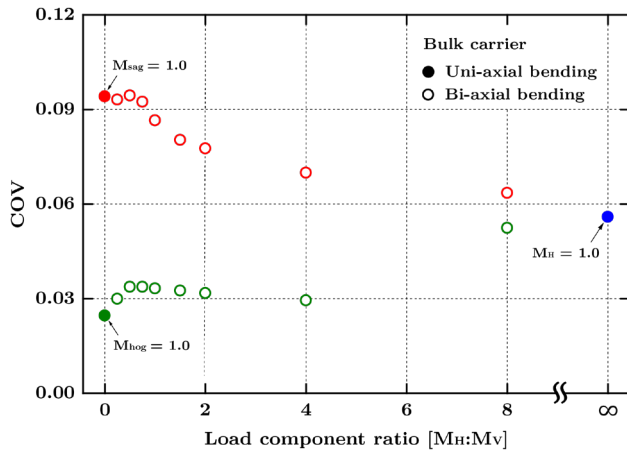


Figure 18(b). Coefficient of variation of ultimate strength under bi-axial load (Bulk carrier)

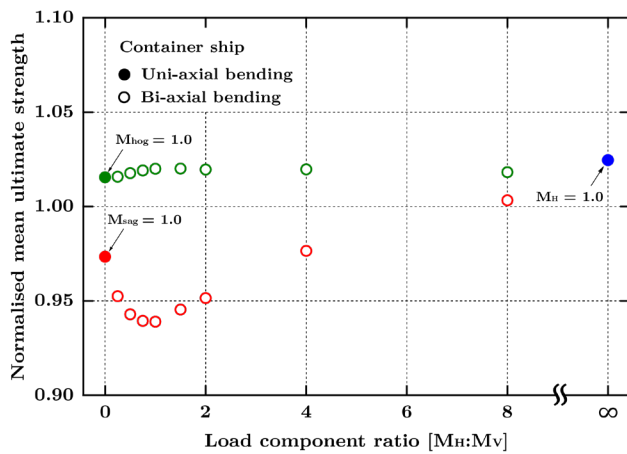


Figure 19(a). Mean ultimate strength under bi-axial load (Container ship)

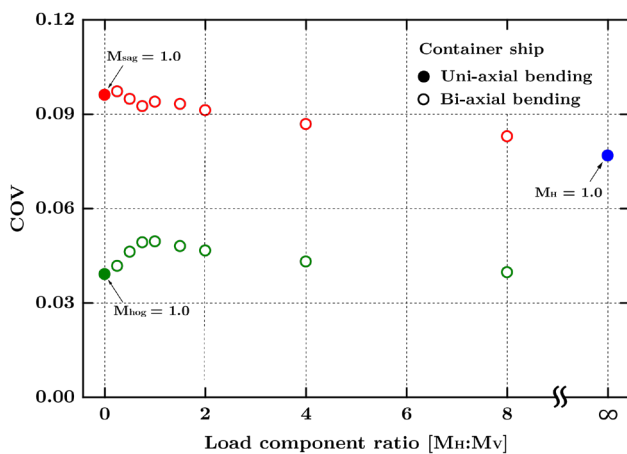


Figure 19(b). Coefficient of variation of ultimate strength under bi-axial load (Container ship)

6. DISCUSSION

It is inevitable that uncertainty exists in the predicted structural capacity of ship hull structures. This is due to the inherent variability of basic variables, and the inadequacy (= inaccuracy) of the engineering model (i.e., model error). Rigorous quantification of the model uncertainty is extremely challenging for ship hull structures because of the limited testing data available, in particular for hull girder systems. However, the computational uncertainty can be evaluated. The computational uncertainty is confined to the uncertainty due to different engineering models for local behaviour modelling, i.e., LSC, which will propagate to the global engineering modelling of ship hull girder strength. In this study, the global engineering model is confined to Smith-type progressive collapse method.

Using a probabilistic approach to four merchant ship models, the present study indicates a considerable variation of ship hull girder strength due to computational uncertainty, i.e., up to 10%. However, this varies substantially between different ship types and different load cases.

The application of the present probabilistic method and the developed data are manifold:

- Incorporation with probabilistic modelling of the basic variables, i.e., ②+④ as shown in Figure 1. This can provide a more reliable estimation of the ultimate bending strength of ship hull girders by improving the characterisation of its probabilistic feature. With the incorporation of an appropriate reliability framework (e.g., first-order reliability method, this will ultimately enhance the reliability and risk assessment of ship hull structures.
- Alternatively, the developed dataset, i.e., mean and COV of the ultimate strength, can be directly applied to the limit state equation as a computational uncertainty factor, provided that the vessel under consideration is of a similar class as those analysed in the present study. However, this will also require an assumption of the probability distribution of this uncertainty factor. As shown in Figure 10 to Figure 13, a normal distribution should be sufficient to describe the hogging strength and horizontal bending strength. On the contrary, a different fitting may be needed for the sagging strength. However, it should be noted that the dominating load cases vary between different ship types. The total bending load consists of a still water component and wave-induced component. Whilst the latter is primarily driven by the dynamic wave-body interaction, the former is caused by the imbalanced distribution of weight and buoyancy, and it is a static design specification for a given loading condition. For instance, container ships are designed to be subjected to hogging load, whereas bulk carriers are prone to sagging failure.

- The present method may also provide validation for new approaches to predict the ultimate bending strength of ship hull girders. Conventionally, the validation of a new method is completed by comparison with experimental data and/or advanced numerical simulation. With the present probabilistic method and the computed mean and COV, one may be able to evaluate whether the new method's result falls into a reasonable interval.

7. CONCLUSIONS

This paper evaluates the computational uncertainty of ship hull ultimate strength predicted by a Smith-type progressive collapse method. In comparison with previous study where only individual influence was considered, this study addresses the combined uncertainty induced by the variance in the structural segment's ultimate compressive capacity and post-collapse characteristics. A novel probabilistic approach integrating the Monte-Carlo Simulation, adaptable LSC algorithm and Smith-type progressive collapse method is adopted, for the first time, to investigate both uniaxial and biaxial load case with combined vertical and horizontal bending of four case study merchant ships. The following conclusions are drawn from the present study:

- The variation in structural components' load-shortening curves could result in a substantial uncertainty in the ultimate ship hull girder strength computed by a Smith-type progressive collapse method.
- In a uniaxial load case, the largest computational uncertainty is induced when the ship hull girder is subjected to sagging. Conversely, the ultimate hogging strength of the ship hull girder is subjected to the smallest computational uncertainty. An intermediate uncertainty is found in the horizontal bending scenario.
- In a bi-axial load case, the computational uncertainty of vertical bending strength is counteracted by horizontal bending. As the latter increases, the uncertainty approaches the one estimated for pure horizontal bending. However, this change is non-proportional with respect to the load component ratio and varies considerably between different ship types.
- The data provided by the present work, i.e., mean and COV of ultimate strength in different load cases, could provide quantitative justification for the selection of strength model error factor in reliability analysis

Within the same context, the research will continue to investigate the effects of the correlation between critical LSC features. An extended case study will be conducted on different ship models in the light of deriving a unified probabilistic model for ship hull girder strength considering computational uncertainty. Regarding the loading scenario, a follow-up study could be conducted for cyclic vertical bending, which can be a typical load

case in the extreme ocean environment. In addition, the application of the uncertainty evaluation procedure will be combined with reliability analysis to elucidate the influence of strength model uncertainty on the safety index of marine structures.

8. ACKNOWLEDGEMENT

This research was supported by Brain Pool program funded by the Ministry of Science and ICT through the National Research Foundation of Korea (2021H1D3A2A02094658).

9. REFERENCES

1. ADAMCHAK, J.C. (1982). *A program for estimating the collapse model of a ship's hull girder under longitudinal bending*. U.S. Navy, Naval Surface Warfare Centre, Carderock Division, David Taylor Naval Ship Research and Development Centre Report 82.076.
2. BENSON, S., DOWNES, J., DOW, R.S. (2013). *Compartment level progressive collapse analysis of lightweight ship structures*. Marine Structures, 31, 44–62.
3. BENSON, S., DOWNES, J., DOW, R.S. (2015). *Overall buckling of lightweight stiffened panels using an adapted orthotropic plate method*. Engineering Structures, 85, 107–117.
4. CALDWELL, J.B. (1965). *Ultimate longitudinal strength*. Transaction of RINA 107, 411–430.
5. DOW, R.S., SMITH, C.S. (1986). *FABSTRAN: A computer program for frame and beam static and transient response analysis (Nonlinear)*. ARE report TR86205.
6. DOW, R.S. (1997). *Structural redundancy and damage tolerance in relation to ultimate ship hull strength*. In Proceeding: Advances in Marine Structures 3, DERA, Dunfermline, Scotland.
7. DOWNES, J., GOKHAN, T.T., ILLIA, K., C. JOONMO, C. (2017). *A new procedure for load shortening and -elongation data for progressive collapse method*. International Journal of Naval Architecture and Ocean Engineering, 9, 705–719.
8. FAULKNER, D.A. (1975). *Review of effective plating for the analysis of stiffened plating in bending and compression*. Journal of Ship Research, 19, 1–17.
9. FRANKLAND, J.M. (1940). *The strength of ship plating under edge compression*. Report 469, U.S. Experimental Modal Basin Navy Yard, Washington D.C., US.
10. FUJIBUBO, M., ALIE, M.Z.M., TAKEMURA, K., IJIMA, K., OKA, S. (2012). *Residual hull girder strength of asymmetrically damaged ships*. Journal of the Japan Society of Naval Architects and Ocean Engineering, 16, 131–140.
11. GASPAR, B., TEIXEIRA, A.P., GUEDES SOARES, C. (2016). *Effect of the Nonlinear*

- Vertical Wave-Induced Bending Moments on the Ship Hull Girder Reliability*. Ocean Engineering, 119, 193–207.
12. GONG, C.Q., FRANGOPOL, D.M. (2020). *Time-variant hull girder reliability considering spatial dependence of corrosion growth, geometric and material properties*. Reliability Engineering & System Safety 193, 106612.
 13. GORDO, J.M., GUEDES SOARES, C. (1996). *Approximate method to evaluate the hull girder collapse strength*. Marine Structures, 9, 449–470.
 14. GUEDES SOARES, C., TEIXEIRA, A.P. (2000). *Structural reliability of two bulk carrier designs*. Marine Structures, 13, 107–128.
 15. ISSC (2000). *Ultimate Strength (Committee III.1)*. The 18th International Ship and Offshore Structures, Nagasaki, Japan.
 16. ISSC (2012). *Ultimate Strength (Committee III.1)*. The 18th International Ship and Offshore Structures, Rostock, Germany.
 17. IACS (2019). *Common structural rules for bulk carriers and oil tankers*. International Association of Classification Societies, London, UK.
 18. KENNEDY, M.C., O'HAGAN, A. (2001). *Bayesian Calibration of Computer Models*. Journal of the Royal Statistical Society, Series B 63(3), 425–464.
 19. KIUREGHIANA, A.D., DITLEVSEN, O. (2009). *Aleatory or Epistemic? Does It Matter?* Structural Safety, 31(2), 105–112.
 20. KIM, D.K., PARK, D.K., KIM, J.H., KIM, S.J., KIM, B.J., SEO, J.K., PAIK, J.K. (2012). *Effect of corrosion on the ultimate strength of double hull oil tankers-Part I: stiffened panels*. Structural Engineering and Mechanics, 42(4), 507–530.
 21. KIM, D.K., KIM, S.J., KIM, H.B., ZHANG, X.M., LI, C.G., PAIK, J.K. (2015). *Ultimate strength performance of bulk carriers with various corrosion additions*. Ships and Offshore Structures, 10(1), 59–78.
 22. KIM, D.K., LIM, H.L., KIM, M.S., HWANG, O.J., PARK, K.S. (2017). *An empirical formulation for predicting the ultimate strength of stiffened panels subjected to longitudinal compression*. Ocean Engineering, 140, 270–280.
 23. KIM, D.K., WONG, E.W.C., LEE, E.B., YU, S.Y., KIM, Y.T. (2019). *A method for the empirical formulation of current profile*. Ships and Offshore Structures, 14(2), 176–192.
 24. LIU Y., FRANGOPOL, D.M. (2018). *Time-dependent reliability assessment of ship structures under progressive and shock deteriorations*. Reliability Engineering & System Safety, 173, 116–128.
 25. LI, S., HU, Z.Q., BENSON, S. (2020a). *The sensitivity of ultimate ship hull strength to the structural component load-shortening curve*. In: Proceedings of 30th International Offshore and Polar Engineering Conference, Shanghai, China.
 26. LI, S., HU, Z.Q., BENSON, S. (2020b). *Progressive collapse analysis of ship hull girders subjected to extreme cyclic bending*. Marine Structures 73, 102803.
 27. LI, S., KIM, D.K., BENSON, S. (2021a). *A probabilistic approach to assess the computational uncertainty of ultimate strength of hull girders*. Reliability Engineering & System Safety, 213, 107688.
 28. LI, S., KIM, D.K., BENSON, S. (2021b). *An adaptable algorithm to predict the load-shortening curves of stiffened panels in compression*. Ships and Offshore Structures, 16:sup1, 122–139.
 29. LI, S., KIM, D.K. (2022). *A comparison of numerical methods for damage index based residual ultimate limit state assessment of grounded ship hulls*. Thin-Walled Structures, 172, 108854.
 30. LIN, Y.T. (1985). *Ship longitudinal strength modelling*. PhD thesis, University of Glasgow.
 31. LIU, B., GUEDES SOARES, C. (2020). *Ultimate strength assessment of ship hull structures subjected to cyclic bending moments*. Ocean Engineering, 215, 107685.
 32. LIU, B., GAO, L., AO, L., WU, W. (2021a). *Experimental and numerical analysis of ultimate compressive strength of stiffened panel with openings*. Ocean Engineering, 220, 108453.
 33. LIU, B., YAO, X., LIN, Y., WU, W., GUEDES SOARES, C. (2021b). *Experimental and numerical analysis of ultimate compressive strength of long-span stiffened panels*. Ocean Engineering, 237, 109633.
 34. MATTHIES, H.G. (2007). *Quantifying Uncertainty: Modern Computational Representation of Probability and Applications*. In: Extreme Man-Made and Natural Hazards in Dynamics of Structures, NATO. Security through Science Series, 105–135 eds: A Ibrahimbegovic and I Kozar. Springer.
 35. PAIK, J.K., MANSOUR, A.E. (1995). *A simple formulation for predicting the ultimate strength of ships*. Journal of Marine Science and Technology, 1, 52–62.
 36. PAIK, J.K., THAYAMBALLI, A.K. (1997). *An empirical formulation for predicting the ultimate compressive strength of stiffened panels*. In: Proceeding: 7th International Offshore and Polar Engineering Conference (ISOPE), 328–338.
 37. PAIK, J.K., THAYAMBALLI, A.K., KIM, B.J. (2001). *Advanced Ultimate Strength Formulations for Ship Plating Under Combined Biaxial Compression/Tension, Edge Shear, and Lateral Pressure Loads*. Marine Technology, 38(1), 9–25.

38. PAIK, J.K. (2006). *The Intelligent Supersize Finite Element Method: Theory and Practice*. Department of Naval Architecture and Ocean Engineering, Pusan National University, Busan, Korea
39. PAIK, J.K., THAYAMBALLI, A.K. (2007). *Ship-Shaped Offshore Installations: Design, Building, and Operation*. Cambridge University Press.
40. PAIK, J.K., MELCHERS, R.W. (2008). *Condition Assessment of Aged Structures*. Woodhead Publishing, Cambridge, UK.
41. PAIK, J.K., KIM, D.K., KIM, M.S. (2009). *Ultimate strength performance of Suezmax tanker structures: pre-CSR versus CSR designs*. International Journal of Maritime Engineering, 151 (Part A2), 39–58.
42. PAIK, J.K., KIM, D.K., PARK, D.H., KIM, H.B., KIM, M.S. (2013). *A new method for assessing the safety of ships damaged by grounding*. International Journal of Maritime Engineering, 154 (Part A1), 1–20.
43. PAIK, J.K. (2018). *Ultimate limit state design of steel-plated structures*. John Wiley Sons, Inc.
44. PAIK, J.K. (2020) *Advanced structural safety studies: with extreme conditions and accidents*. Springer.
45. PARUNOV, J., GUEDES SOARES, C. (2008). *Effects of Common Structural Rules on hull-girder reliability of an Aframax oil tanker*. Reliability Engineering & System Safety, 93(9), 1317–1327.
46. PARUNOV, J., PREBEG, P., RUDAN, S. (2020). *Post-accidental structural reliability of double-hull oil tanker with near realistic collision damage shapes*. Ships and Offshore Structures, 15:sup1, 190–207.
47. RINGSBERG, J.W., DARIE, I., NAHSHON, K., SHILLING, G., VAZ, M.A., BENSON, S., BRUBAK, L., FENG, G.Q., FUJIKUBO, M., GAIOTTI, M., HU, Z.Q. JANG, B.S., PAIK, J.K., SLAGSTAD, M., TABRI, K., WANG, Y.K., WIEGARD, B., YANAGIHARA, D. (2021). *The ISSC 2022 committee III.1: ultimate strength benchmark study on the ultimate limit state analysis of a stiffened plate structure subjected to uniaxial compressive loads*. Marine Structures, 79, 103026.
48. SMITH, C.S. (1977). *Influence of local compressive failure on ultimate longitudinal strength of a ship's hull*. In: Proceedings of International Symposium on Practical Design of Ships and others Floating Structures, Tokyo, Japan.
49. SYRIGOU, M., BENSON, S.D., DOW, R.S. (2018). *Progressive collapse assessment of intact box girders under combined bending and torsional loads*. In: Proceedings of International Conference on Ships and Offshore Structures (ICSOS 2018), Gothenburg, Sweden.
50. TEIXEIRA, A.P., GUEDES SOARES, C. (2009). *Reliability analysis of a tanker subjected to combined sea states*. Probabilistic Engineering Mechanics, 24, 493–503.
51. TATSUMI, A., KO, H., FUJIKUBO, M. (2020). *Ultimate strength of container ships subjected to combined hogging moment and bottom local loads part 2: An extension of Smith's method*. Marine Structures, 71, 102738.
52. XU, M.C, TEIXEIRA, A.P., GUEDES SOARES, C. (2015). *Reliability assessment of a tanker using the model correction factor method based on the IACS-CSR requirement for hull girder ultimate strength*. Probabilistic Engineering Mechanics, 42, 42–53.
53. XU, MC, SONG, ZJ, ZHANG, BW, PAN, J. (2018). *Empirical formula for predicting ultimate strength of stiffened panel of ship structure under combined longitudinal compression and lateral loads*. Ocean Engineering, 162, 161–175.
54. YAO, T., NIKOLOV, P. (1991). *Progressive collapse analysis of a ship's hull under longitudinal bending (1st report)*. Journal of the Society of Naval Architects of Japan, 170, 449–461.
55. YAO, T, NIKOLOV, P. (1992). *Progressive collapse analysis of a ship's hull under longitudinal bending (2nd report)*. Journal of the Society of Naval Architects of Japan, 172, 437–446.
56. YOUSSEF, S.A.M., FAISAL, M., SEO, J.K., KIM, B.J., HA, Y.C., KIM, D.K., PAIK, J.K., CHENG, F., KIM, M.S. (2016). *Assessing the risk of ship hull collapse due to collision*. Ships and Offshore Structures, 11(4), 335–350.
57. ZHANG, S., KHAN, I. (2009). *Buckling and ultimate capability of plates and stiffened panels in axial compression*. Marine Structures, 22, 791–808.

10. APPENDIX

Normal distribution

$$f(x) = \frac{1}{B\sqrt{2\pi}} \exp\left[-\frac{(x-A)^2}{2B^2}\right]$$

Log-normal distribution

$$f(x) = \frac{1}{xB\sqrt{2\pi}} \exp\left[-\frac{(\ln x - A)^2}{2B^2}\right]$$

2-Parameter exponential distribution

$$f(x) = \frac{1}{A} \exp\left(-\frac{x-B}{A}\right)$$

Smallest extreme value distribution

$$f(x) = \frac{1}{B} \exp\left(\frac{x-A}{B}\right) \exp\left[-\exp\left(\frac{x-A}{B}\right)\right]$$

3-Parameter Weibull distribution

$$f(x) = \frac{B}{A} \left(\frac{x-C}{A}\right)^{B-1} \exp\left[-\left(\frac{x-C}{A}\right)^B\right]$$

Largest extreme value distribution

$$(A1) \quad f(x) = \frac{1}{B} \exp\left(-\frac{x-A}{B}\right) \exp\left[-\exp\left(\frac{x-A}{B}\right)\right] \quad (A6)$$

Logistic distribution

$$(A2) \quad f(x) = \frac{\exp\left(\frac{x-A}{B}\right)}{B \left[1 + \exp\left(\frac{x-A}{B}\right)\right]^2} \quad (A7)$$

Log-logistic distribution

$$(A3) \quad f(x) = \frac{\exp\left(\frac{\ln x - A}{B}\right)}{Bx \left[1 + \exp\left(\frac{\ln x - A}{B}\right)\right]^2} \quad (A8)$$

3-Parameter log-logistic distribution

$$(A5) \quad f(x) = \frac{\exp\left(\frac{\ln(x-C)-A}{B}\right)}{B(x-C) \left[1 + \exp\left(\frac{\ln(x-C)-A}{B}\right)\right]^2} \quad (A9)$$

